



Permafrost siderite reveals a hidden climate-sensitive inorganic carbon reservoir

Fernando Montaña-López^{1,2+}, Ravi Kukkadapu³⁺, Sean R. Schaefer^{4,5}, Jessica Gilman Ernakovich^{5,6}, and Caitlin Hicks Pries^{1,2}.

5 ¹ Ecology, Evolution, Environment and Society Program, Dartmouth College, Hanover, New Hampshire, 03755, USA

² Department of Biological Sciences, Dartmouth College, Hanover, New Hampshire, 03755, USA

³ Environmental Molecular Sciences Laboratory, Earth and Biological Sciences Directorate, Pacific Northwest National Laboratory, Richland, WA 99352, USA

⁴ Natural Resources and Earth Systems Science Program, University of New Hampshire, Durham, NH, 03824, USA.

10 ⁵ Center of Soil Biogeochemistry and Microbial Ecology (Soil BioME), University of New Hampshire, Durham, NH, 03824, USA.

⁶ Department of Natural Resources and the Environment, University of New Hampshire, Durham, NH, 03824, USA.

⁺These authors contributed equally to this work

15 *Correspondence to:* Caitlin Hicks Pries (caitlin.hicks.pries@dartmouth.edu), Fernando Montaña-López (fernando.gr@dartmouth.edu)

Abstract. We report direct evidence of an inorganic carbon pool that is sensitive to permafrost thaw—siderite. Notably, siderite was absent in the seasonally thawed active layer above permafrost, implying this inorganic carbon reservoir may be lost upon thaw. Assuming siderite weathers quickly once permafrost thaws, we estimate siderite weathering could release
20 carbon equivalent to about 10% of permafrost organic carbon losses over the next half-century. However, studies are needed to understand how widespread siderite is and to quantify its actual weathering rate. This study is submitted as a LESSONS Report because it documents a surprise result that opens up opportunities for new science.

1 Main text

The large stores of organic carbon in permafrost and their potential to become a positive feedback to climate change are well
25 recognized. It is estimated that permafrost contains roughly 1600 Pg of organic carbon, approximately twice as much carbon as the entire atmosphere (Schuur et al., 2022). This organic carbon has built up over thousands of years as freezing temperatures have limited microbial decomposition; but, in the coming decades to centuries, permafrost thaw will likely lead to the loss of 5 to 15% of this organic carbon pool (Schuur et al., 2022). During analyses conducted to investigate organo-mineral interactions in permafrost (Montaña López et al., 2026b), we identified an inorganic form of climate-sensitive
30 permafrost carbon that has heretofore been overlooked—siderite.

Siderite is an iron (II) carbonate mineral (FeCO₃) commonly formed authigenically in anaerobic sediments across geologic time and in the modern day. Modern siderite formation occurs in freshwater swamps and bogs with high ferrous iron



35 concentrations and low sulfate and chloride concentrations (Postma, 1980, 1982), peat (McMillan and Schwertmann, 1998),
and lake sediments (Vuillemin et al., 2019). Modern siderite can form through the microbially-mediated dissimilatory
reduction of ferric oxyhydroxides using organic matter (OM) under anoxic conditions, which contributes both the Fe(II) and
CO₃²⁻ necessary to form siderite via precipitation (Postma, 1982). Here we show, for the first time, direct evidence of siderite
in Arctic permafrost.

40 Siderite was detected in permafrost soils from four different sites across the North Slope of Alaska using Mössbauer
spectroscopy. These sites were chosen for their variability in parent material and age since deglaciation, which led to a range
in pH, organic and inorganic carbon content (Table 1). Table 1 reports only the subset of samples analyzed by Mössbauer
spectroscopy, which are part of a larger dataset of ~250 permafrost soil samples with broader chemical characterization
(Montaño López et al., 2026b). The room temperature (RT) Mössbauer spectra revealed a distinct Fe(II) doublet with
45 parameters (CS (center shift) = 1.24-1.27 mm/sec and QS (quadrupole splitting parameter) = 1.82-1.84 mm/sec)
characteristic of natural siderites (Gil-Crespo et al., 1992; Ristić et al., 2017) (Fig. 1A, Fig. A1A). This feature was notably
absent in soils from the mineral active layer (MAL) (Fig. 1B, Fig. A1B). The identification was further confirmed with the
absence or substantial decrease of this feature following a sodium acetate extraction of the soils (Fig. A2), which selectively
dissolves iron carbonate minerals while preserving other iron phases (Poulton and Canfield, 2005). Across these soils, the
50 siderite-associated Fe ranged from about 6.5 to 17% of the total Fe content and siderite content ranged from 0.44 to 1.1% of
soil mass. Previous studies have suggested the presence of siderite in permafrost from porewater analyses (Jessen et al.,
2014) and sequential extractions (Jones et al., 2020; Lipson et al., 2010). One study confirmed its presence in permafrost of
mafic parent material using X-ray diffraction (XRD) (Chen, 2025). To our knowledge, this marks the first direct observation
of siderite in non-mafic permafrost, offering evidence that this previously unaccounted inorganic permafrost carbon pool
55 might be broadly distributed. This is also the first study to note its absence from adjacent mineral active layers.

Table 1. Chemical characteristics of permafrost soils in this study. Values represent averages ± standard errors of analytical replicates where available.

Site	Depth (cm)	pH	Total Fe (%)	Siderite (%)	Siderite-Fe (% of Fe)	Organic carbon (%)	Inorganic carbon (%)
Itkillik II	55-60	5.41 ± 0.06	4.21	1.06	12.2	3.41 ± 0.11	trace
Itkillik I	50-73	5.29 ± 0.01	4.59	0.67	7.0	3.97 ± 0.28	trace
Sagavanirktok	42-53	4.82 ± 0.09	3.25	0.44	6.5	4.44 ± 0.06	trace
Unglaciated	79-100	7.61 ± 0.03	2.88	1.02	17.0	3.97 ± 0.12	1.21 ± 0.10

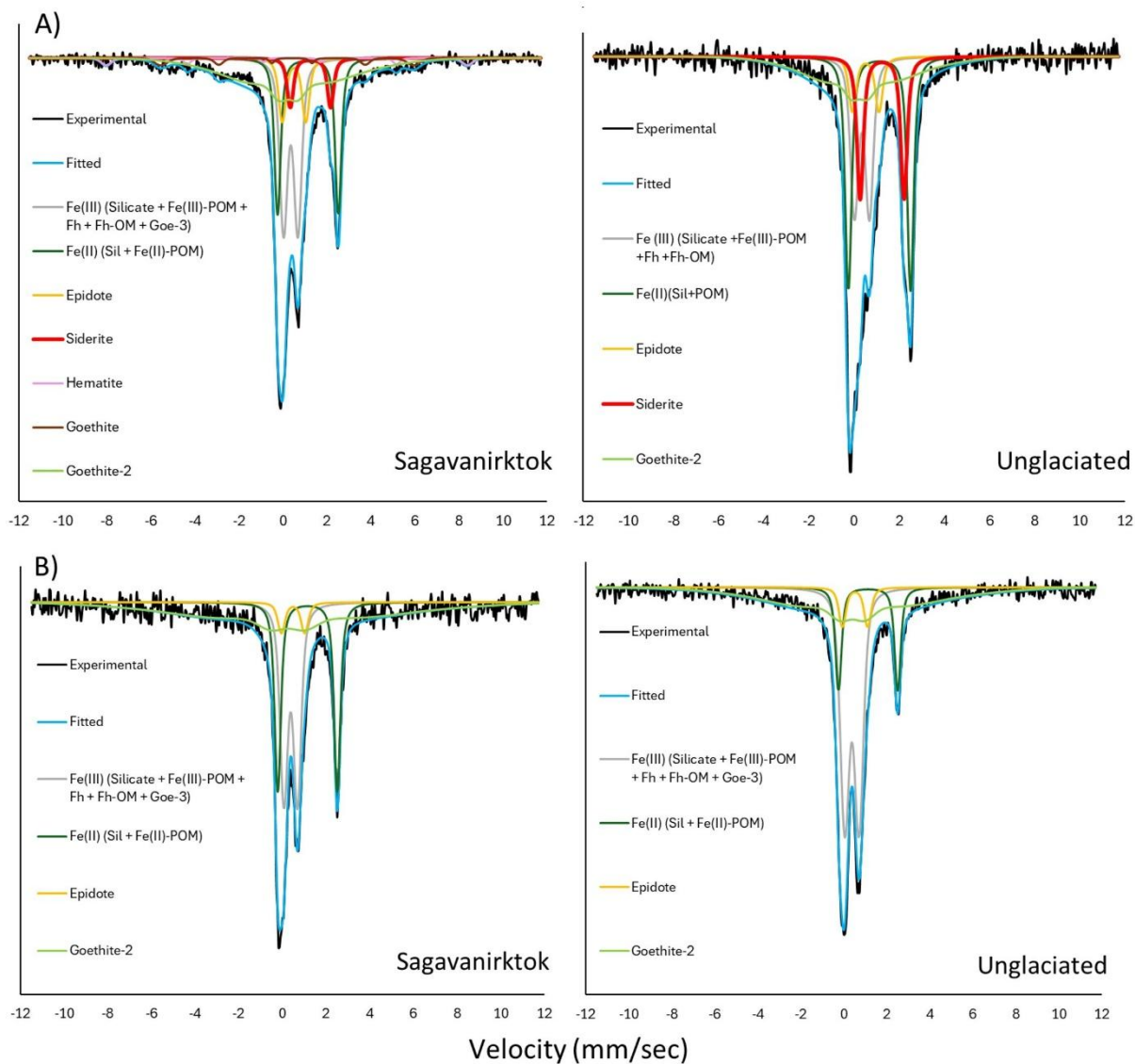


Figure 1. Fitted Mössbauer spectra of two permafrost soils (A) and their corresponding mineral active layers (B) at room temperature (RT). The siderite doublet feature is highlighted in red for clarity. The absence of the siderite doublet feature reflects its loss through dissolution under variable redox conditions. These sites represent the pH extremes of the study (Sagavanirktok pH = 4.82; Unglaciated pH = 7.61); spectra from other sites are provided in the supporting information (Fig. A1).

Mössbauer spectroscopy is the preferred method to identify small amounts of siderite (<1 wt.%) that are undetectable using XRD; accordingly, siderite was not observed in our XRD analyses (Montaño López et al., 2026b). Identification is likewise challenging using electron microscopy and iron extended X-ray absorption fine structure spectroscopy (Fe-EXAFS), where Fe(II) phases in permafrost consistent with siderite have been previously suggested but not conclusively identified (Joss et



al., 2022; Sowers et al., 2020). In this study, each sample was analyzed once by Mössbauer spectroscopy, consistent with the common workflow for mineral phase identification in complex natural matrices, where constraints such as low throughput and significant measurement time preclude routine analytical replication (Bhattacharyya et al., 2022; Chen et al., 2015; 80 Kukkadapu et al., 2001; Thompson et al., 2025). Instead, robustness is typically assessed through spectral fit quality and consistency across samples, in combination with environmental context and complementary analyses that help to identify specific Fe phases (Bhattacharyya et al., 2022; Chen et al., 2015; Kukkadapu et al., 2001; Thompson et al., 2025).

The wide range of pH and total inorganic carbon content of our permafrost soils suggest that the siderite formed 85 authigenically and was not inherited from the parent material (Table 1). Three of our soils had pH values lower than 6, deviating strongly from the typical soil carbonate baseline (pH >7.5) (Loeppert and Suarez, 1996), and contained only trace amounts of inorganic carbon (siderite IC was <0.11 wt %). In contrast, one soil with a pH around 7.3 exhibited effervescence when treated with dilute HCl and had measurable amounts of inorganic carbon (1.2%) based on thermal mass loss between 600-1000 °C, during which carbonate minerals breakdown (Vuong et al., 2013). While the pH of the latter site could suggest 90 that its parent material influenced siderite formation (because carbonates can enhance the formation of siderite (Roh et al., 2003)), the presence of siderite in acidic pH environments indicates that its formation was likely driven by in situ biogeochemical processes and not the parent material (Grengs et al., 2024; Sánchez-Román et al., 2014).

The freezing and reducing conditions characteristic of permafrost soils provide the geochemical environment required for 95 siderite formation; however, the actual mechanisms and extent of siderite formation in permafrost are unclear and warrant further investigation. The formation of siderite generally relies on three key factors: 1) a supply of Fe, 2) high concentrations of carbon dioxide or carbonates, and 3) anaerobic conditions (Fredrickson et al., 1998). As in most soils, weathering processes actively break down parent materials, providing the Fe. This Fe, typically in the Fe(III) form, is reduced to Fe(II) under the anoxic conditions found in permafrost, where ice-rich layers can restrict gas diffusion and help maintain low-redox 100 conditions (Martz et al., 2016). At the same time, microbial decomposition of OM in permafrost releases CO₂, raising its partial pressure within the soil's pore space. The resulting rise in dissolved inorganic carbon concentrations favors the precipitation of carbonate minerals like siderite (Xiong et al., 2017). Siderite has also been shown to form in localized zones of active OM degradation, where microbial communities facilitate Fe(III) reduction, promoting the formation of Fe(II) necessary for siderite precipitation (Bukin et al., 2025). Moreover, the high OM content in permafrost may contribute to 105 siderite stability, as functional groups derived from OM can interact with the mineral surface via ligand sorption (Rothwell et al., 2025).

Notably, siderite was absent in mineral active layer soils (Fig. 1B), indicating it was mobilized or transformed during permafrost thaw. While the specific mechanism for siderite weathering in permafrost systems is unknown, thaw-induced 110 shifts from hypoxic (permafrost) to more variable redox conditions (Rooney et al., 2024) likely promote the oxidation of



Fe(II) to Fe(III), leading to the siderite weathering. The products of siderite weathering include carbonate and Fe oxyhydroxides (Frisbee and Hossner, 1995; McMillan and Schwertmann, 1998). The loss of siderite could have implications for organic carbon storage as the resulting reactive Fe(III) ions and Fe oxides could subsequently promote OM protection via complexes and sorption (Rothwell et al., 2025). In contrast, the associated carbonate ions released into solution could
115 directly contribute to CO₂ losses, depending on the pH of the soil solution and the conditions of the carbonate equilibrium.

We ran a thought experiment to estimate the amount of inorganic carbon that could be released into the soil solution when permafrost thaws and siderite weathers. Using the average bulk Fe and siderite-Fe content of our soils, which are 3.7% and 11% (Table 1), respectively, and a typical bulk density of Alaskan mineral permafrost of 0.89 g soil cm⁻³ (Ainuddin et al.,
120 2024), the soils contain about 0.76 mg (range 0.40 to 0.98 mg) of siderite carbon in each cubic centimeter. If we assume that permafrost thaws at a rate of 0.11 cm per year (Liu et al., 2024), then siderite weathering leads to 0.84 g C m⁻² (range 0.44 to 1.1 g C m⁻²) becoming vulnerable to loss each year as dissolved bicarbonate ions or CO₂, depending on the carbonate equilibrium. At a soil solution pH of 4.3, almost 100% of this inorganic carbon could be in the form of dissolved CO₂, while 0% would be in the form of CO₂ at a soil solution pH of 8.2 (Zosel et al., 2011), the pH of our active layers ranges from 5 to
125 6. To put this estimate of inorganic carbon released from siderite in perspective, our soils have an average organic carbon content of 3.9% (range 3.4 to 4.4%), assuming that 22% of mineral soil carbon is likely to be mineralized over 50 years (based on an incubation meta-analysis (Schädel et al., 2014)), 8.5 g C m⁻² could be lost from organic matter for each 0.11 cm of thaw. The mobilization of siderite carbon is thus equivalent to 9.8% (range 4.7 to 14.7%; Table A1) of the loss of organic carbon over 50 years. While this time period seems reasonable, it should be noted that the actual rate of siderite weathering
130 upon permafrost thaw is unknown. We caution that this calculation is highly simplified and should be interpreted as a first-order estimate, as it assumes uniform thaw, average soil properties, and complete siderite weathering, all of which remain uncertain in permafrost environments.

Siderite may be widespread in permafrost, given that we found it across Alaska's North Slope in soils with wide-ranging pH
135 values, and that siderite indicators have previously been documented in Iceland (Chen, 2025), Greenland (Jessen et al., 2014), and Svalbard (Jones et al., 2020). Siderite, therefore, represents a small but significant carbon pool in permafrost that warrants further study. Future research should aim to quantify siderite pools across permafrost soils, test the rate and controls of siderite weathering upon thaw, and trace the fate of siderite carbon after its transformation to dissolved inorganic carbon, whether it be outgassed as CO₂ or transported to ground and surface water. Accounting for these processes in Earth system
140 models may be vital to refining projections of permafrost-climate feedback.

2 Materials and Methods

Our sites were located along the North Slope, Alaska in the foothills of the Brooks Range from south of Toolik Lake through the Sagwon Hills about 100 km to Toolik's north. We chose the sites based on the glacial drift on which they were located—



145 Itkillik II (~11.5-25 ka), Itkillik I (~53-66 ka), Sagavanirktok (~125-728 ka), and Unglaciaded (4.5 Ma). These drifts
represent not only a gradient in time since deglaciation but also differences in parent material (Ping et al., 1998; Walker et
al., 1998). The parent materials vary from acidic glacial till in the younger drifts (Itkillik II, Itkillik I and Sagavanirktok), to
near-neutral calcareous loess-dominated surfaces in the oldest site (Unglaciaded). The youngest landscape was situated at 893
meters above sea level while the oldest was at 214, with slopes ranging from 3.3 to 4.8 degrees. Soil cores were collected in
August of 2021 and 2022 when the active layer was approaching peak seasonal thaw depth. We sampled from the surface to
150 depths averaging 68 cm, with core lengths ranging from 52-109 cm depending on site conditions, with the goal of sampling
below the permafrost-active layer interface across our four sites. Seasonally thawed (mineral active layer) soils were first
sampled by cutting rectangular blocks of soil with a knife, with samples collected from 20-38 cm below the soil surface for
this study. Then we used a Snow, Ice and Permafrost Research Establishment (SIPRE) corer to sample frozen soils below.
Permafrost soil depths are given in Table 1. Soils were immediately stored on dry ice and were transported frozen from the
155 field sites to the laboratory.

We measured pH using a 1:2 soil-to-water ratio (Mettler Toledo S220 pH/ion meter). A multiphase carbon determinator
(MCD, RC612, Leco, St. Joseph, MI, USA) was used for simultaneous analysis of soil organic and inorganic carbon by
thermal analysis. The MCD temperature increased from 140 to 1000°C over 30 minutes using O₂ as the carrier gas. The CO₂
160 evolved during heating was quantified by infrared detection at a frequency of three measurements per second. Based on the
isolated peaks, CO₂ released above 600 °C was assigned to soil inorganic carbon (SIC)(Natali et al., 2020; Vuong et al.,
2013). Calibration was performed using certified CaCO₃ standards (Alpha Resources 1034) containing 1 and 12% carbon,
which served as the reference materials.

165 Mössbauer spectra to characterize and quantify Fe-species were collected on mineral active layer and permafrost soils from
our four sites (Itkillik II, Itkillik I, Sagavanirktok, and Unglaciaded). Additionally, two permafrost soils with enhanced
siderite content (Itkillik II and Unglaciaded) were analyzed post-sodium acetate extraction (described below) to confirm the
absence of siderite features after treatment. Mössbauer spectra were collected using a 75 millicurie (initial strength) ⁵⁷Co/Rh
source. A velocity transducer (WissEl Elektronik, Germany) was operated in a constant acceleration mode (23 Hz, ±12
170 mm/sec). An Ar-Kr proportional counter was used to detect the radiation transmitted through the sample, and the counts
were stored as a function of energy (transducer velocity, 1024 channels). Raw data were folded into 512 channels to provide
a flat background and a zero-velocity position corresponding to the center shift of an iron foil (7-micron-thick α-Fe(m) foil;
Amersham, England). The experimental data were modeled with Recoil software using a Voigt-based structural fitting
routine(Rancourt and Ping, 1991).

175

To dissolve carbonate-associated Fe in soil, we followed the method from (Poulton and Canfield, 2005), briefly we shook
0.25 g of finely ground soil with 12.5 mL of 1 M sodium acetate solution adjusted (with acetic acid) to pH 4.5 at room



temperature for 48 hours and then centrifuged samples at 20,000 xG for 20 minutes, suspensions were filtered through Whatman 52 filter papers and the remaining pellets were sent for Mössbauer spectroscopy analysis.

180

To analyze total iron, soil samples (~3g) were submitted to Activation Laboratories Ltd. (Actlabs, Canada), an International Organization for Standardization (ISO) 17025-accredited commercial laboratory for geochemical analysis. The samples were finely ground, and the loss on ignition was determined. A representative subsample was fused with lithium metaborate/tetraborate flux, then digested in weak HNO₃ solution. The resulting solution was analyzed for total elements using inductively coupled plasma-optical emission spectroscopy (ICP-OES), following the Actlabs “4B Geochemistry” analytical package (ACTLABS, 2025).

185

190

195

200

205



Appendix A

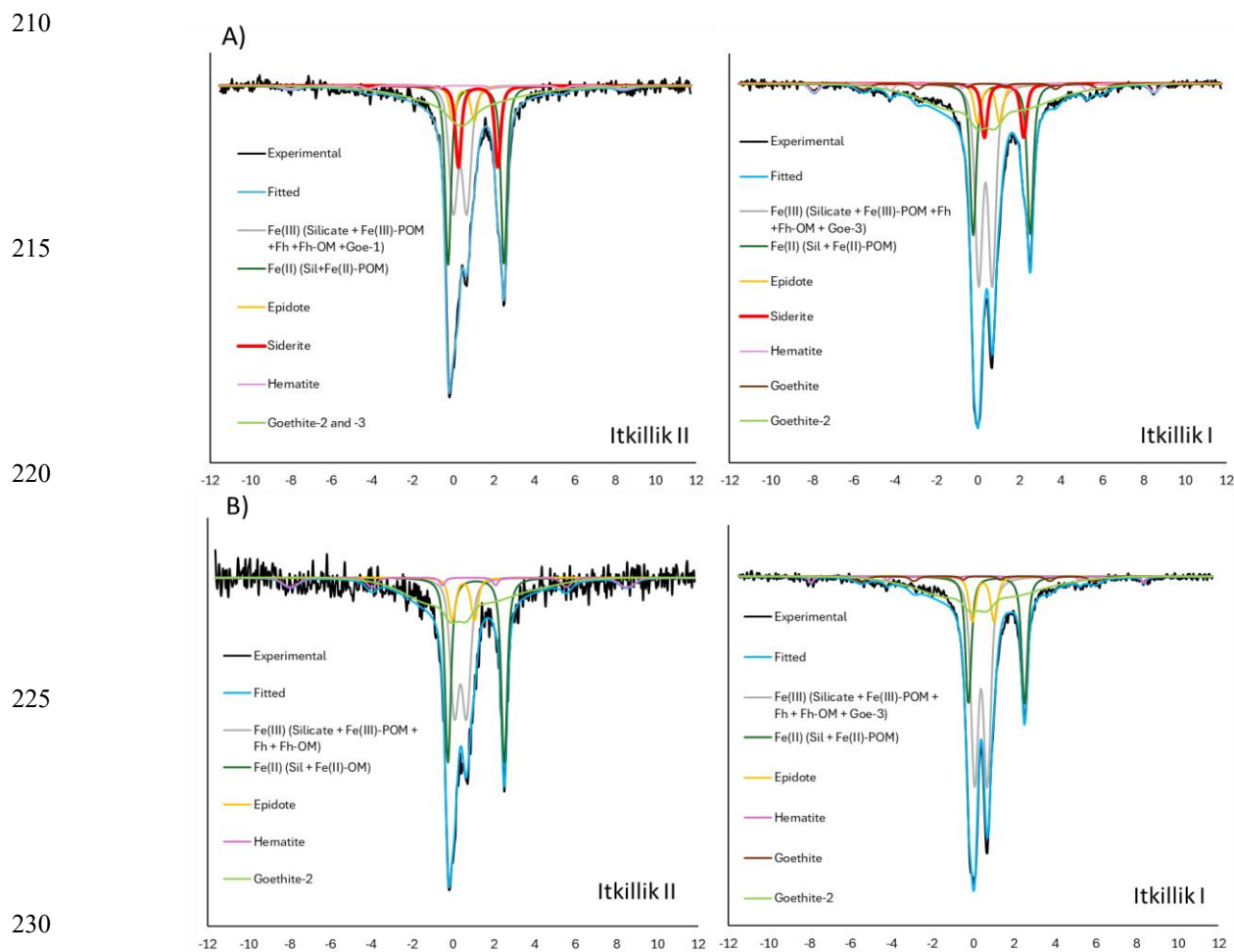


Figure A1. Fitted Mössbauer spectra of the two remaining permafrost soils (A) and their corresponding mineral active layers (B) at room temperature (RT). The siderite doublet feature is highlighted in red for clarity. The absence of the siderite doublet feature reflects its loss through dissolution under variable redox conditions.

235

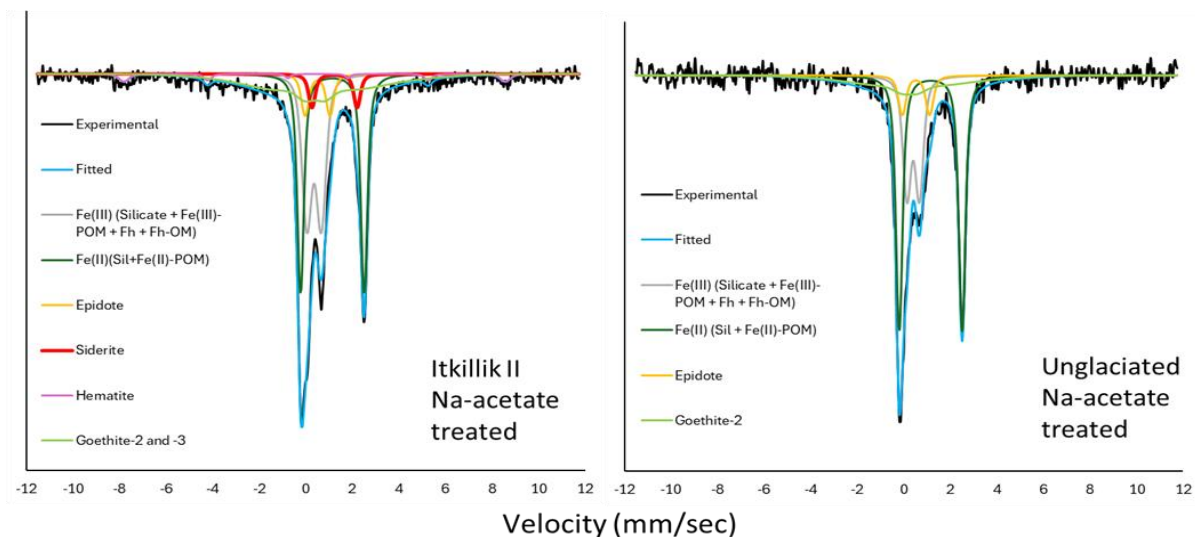


Figure A2. Fitted Mössbauer spectra (measured at RT) of two permafrost samples with elevated siderite content after sodium acetate treatment. The siderite doublet feature is diminished in the Itkillik II sample, indicating partial dissolution, while the Unglaciaded sample showed complete dissolution of siderite.

240

Table A1. Geochemical values from our sites and constants from the literature (footnote) used to estimate siderite-derived carbon loss upon permafrost thaw and to compare its magnitude with potential organic carbon losses.

Site	Total Fe (%)	Siderite-Fe (% of Fe)	TOC (%)	Siderite (mg g ⁻¹ soil)	Siderite-Fe (mg Fe cm ⁻³)	Siderite-C (mg C cm ⁻³)	Siderite loss (g C m ⁻² y ⁻¹)	OC loss (g C m ⁻² y ⁻¹)	% of OC loss
Itkillik II	4.21	12.2	3.41	10.65	4.571	0.983	1.08	7.34	14.7
Itkillik I	4.6	7.0	3.97	6.68	2.866	0.616	0.678	8.55	7.9
Sagavanirktok	3.25	6.5	4.44	4.38	1.880	0.404	0.445	9.56	4.7
Unglaciaded	2.88	17	3.97	10.2	4.357	0.937	1.03	8.55	12.1
<i>Mean</i>	<i>3.74</i>	<i>10.7</i>	<i>3.95</i>	<i>8.27</i>	<i>3.55</i>	<i>0.763</i>	<i>0.839</i>	<i>8.50</i>	<i>9.8</i>

245 Constants used: thaw rate = 0.11 cm yr⁻¹ (Liu et al., 2024); bulk density = 0.89 g soil cm⁻³ (Ainuddin et al., 2024); OC loss = 22% respired over 50 years (Schädel et al., 2014); siderite molar mass = 115.848 g mol⁻¹; Fe molar mass = 55.85 g mol⁻¹.

Data availability

All data needed to evaluate the conclusions in the paper are present in the paper and/or the Appendix. Raw data are publicly available online at (Montaño López et al., 2026a) <https://doi.org/10.18739/A2R49GB9D>



Author contributions

250 Conceptualization: CHP, RK, FML. Data and formal analysis: RK, CHP, FML. Funding acquisition: CHP, JGE, FML, SRS.
Investigation: all authors. Methodology: RK, FML, CHP. Project administration: CHP. Supervision: CHP. Visualization:
FML, RK. Writing—original draft: FML, CHP, RK. Writing—review & editing: all authors.

Competing interests

The authors declare that they have no competing interests.

260 Acknowledgements

We acknowledge the importance of preserving natural areas and honouring the stewardship of their local communities. All research activities were conducted in accordance with relevant review procedures and permitting requirements designed to protect natural environments. We took care to minimize the impact of our sampling efforts. We would like to thank Sarah Goldsmith and Else Schlermann for helping in collection efforts, and Hermann F. Jungkunst, Gesine Preuß, and Caroline

265 Nein for their assistance with thermal analysis.

Financial support

This work was supported by the National Science Foundation, Office of Polar Programs, Grant #2031072 and the Environmental Molecular Sciences Laboratory (for Mössbauer spectroscopy measurements), a DOE Office of Science User Facility sponsored by the FICUS Research program under Project ID 60871.

270 References

ACTLABS: Litho geochemistry, <https://actlabs.com/geochemistry-analysis/litho geochemistry-and-whole-rock-analysis/litho geochemistry-litho/>, 2025.

Ainuddin, I. H., Jelinski, N. A., Matamala, R., Ping, C. L., and Jastrow, J. D.: Soil Carbon and Nitrogen Stocks Across



- Hillslopes Underlain by Continuous Permafrost in the Northern Arctic Foothills, Alaska, United States, *Permafr. Periglac. Process.*, 35, 504–522, <https://doi.org/10.1002/ppp.2244>, 2024.
- 275 Bhattacharyya, A., Kukkadapu, R. K., Bowden, M., Pett-Ridge, J., and Nico, P. S.: Fast redox switches lead to rapid transformation of goethite in humid tropical soils: A Mössbauer spectroscopy study, *Soil Sci. Soc. Am. J.*, 86, 264–274, <https://doi.org/10.1002/SAJ2.20382>, 2022.
- Bukin, S. V., Lomakina, A. V., Pogodaeva, T. V., Khlystov, O. M., Zemsкая, T. I., and Krylov, A. A.: Possible Role of
280 Microbial Communities of Lake Baikal Bottom Sediments in Formation of Authigenic Siderites Anomalously Enriched in ¹³C Isotope, *Microbiology*, 94, 658–675, <https://doi.org/10.1134/S0026261725600806>, 2025.
- Chen, C., Kukkadapu, R., and Sparks, D. L.: Influence of Coprecipitated Organic Matter on Fe²⁺(aq)-Catalyzed Transformation of Ferrihydrite: Implications for Carbon Dynamics, *Environ. Sci. Technol.*, 49, 10927–10936, <https://doi.org/10.1021/ACS.EST.5B02448>, 2015.
- 285 Chen, Z.: Iron-mediated Biogeochemical Cycling of Carbon in (sub-) Arctic Soils, Freie Universität Berlin, 2025.
- Fredrickson, J. K., Zachara, J. M., Kennedy, D. W., Dong, H., Onstott, T. C., Hinman, N. W., and Li, S.: Biogenic iron mineralization accompanying the dissimilatory reduction of hydrous ferric oxide by a groundwater bacterium, *Geochim. Cosmochim. Acta*, 62, 3239–3257, [https://doi.org/10.1016/S0016-7037\(98\)00243-9](https://doi.org/10.1016/S0016-7037(98)00243-9), 1998.
- Frisbee, N. M. and Hossner, L. R.: Siderite Weathering in Acidic Solutions under Carbon Dioxide, Air, and Oxygen, *J. Environ. Qual.*, 24, 856–860, <https://doi.org/10.2134/jeq1995.00472425002400050010x>, 1995.
- 290 Gil-Crespo, P., Pesquera, A., and Velasco Roldán, F.: X-ray Diffraction, Infrared and Mossbauer Studies of Fe-rich Carbonates., *Eur. J. Mineral.*, 4, 521–526, <https://doi.org/10.1127/ejm/4/3/0521>, 1992.
- Grengs, A., Ledesma, G., Xiong, Y., Katsev, S., Poulton, S. W., Swanner, E. D., and Wittkop, C.: Direct precipitation of siderite in ferruginous environments, *Geochemical Perspect. Lett.*, 30, 1–6, <https://doi.org/10.7185/GEOCHEMLET.2414>,
295 2024.
- Jessen, S., Holmslykke, H. D., Rasmussen, K., Richardt, N., and Holm, P. E.: Hydrology and pore water chemistry in a permafrost wetland, Ilulissat, Greenland, *Water Resour. Res.*, 50, 4760–4774, <https://doi.org/10.1002/2013WR014376>, 2014.
- Jones, E. L., Hodson, A. J., Thornton, S. F., Redeker, K. R., Rogers, J., Wynn, P. M., Dixon, T. J., Bottrell, S. H., and O’Neill, H. B.: Biogeochemical Processes in the Active Layer and Permafrost of a High Arctic Fjord Valley, *Front. Earth Sci.*, Volume 8-, 2020.
- 300 Joss, H., Patzner, M. S., Maisch, M., Mueller, C. W., Kappler, A., and Bryce, C.: Cryoturbation impacts iron-organic carbon associations along a permafrost soil chronosequence in northern Alaska, *Geoderma*, 413, 115738, <https://doi.org/10.1016/j.geoderma.2022.115738>, 2022.
- Kukkadapu, R. K., Zachara, J. M., Smith, S. C., Fredrickson, J. K., and Liu, C.: Dissimilatory bacterial reduction of Al-substituted goethite in subsurface sediments, *Geochim. Cosmochim. Acta*, 65, 2913–2924, [https://doi.org/10.1016/S0016-7037\(01\)00656-1](https://doi.org/10.1016/S0016-7037(01)00656-1), 2001.
- 305 Lipson, D. A., Jha, M., Raab, T. K., and Oechel, W. C.: Reduction of iron (III) and humic substances plays a major role in



- anaerobic respiration in an Arctic peat soil, *J. Geophys. Res. Biogeosciences*, 115, <https://doi.org/10.1029/2009JG001147>, 2010.
- 310 Liu, Z., Kimball, J. S., Ballantyne, A., Watts, J. D., Natali, S. M., Rogers, B. M., Yi, Y., Klene, A. E., Moghaddam, M., Du, J., and Zona, D.: Widespread deepening of the active layer in northern permafrost regions from 2003 to 2020, *Environ. Res. Lett.*, 19, 14020, <https://doi.org/10.1088/1748-9326/ad0f73>, 2024.
- Loeppert, R. H. and Suarez, D. L.: Carbonate and Gypsum, in: *Methods of Soil Analysis*, 437–474, <https://doi.org/10.2136/sssabookser5.3.c15>, 1996.
- 315 Martz, F., Vuosku, J., Ovaskainen, A., Stark, S., and Rautio, P.: The Snow Must Go On: Ground Ice Encasement, Snow Compaction and Absence of Snow Differently Cause Soil Hypoxia, CO₂ Accumulation and Tree Seedling Damage in Boreal Forest, *PLoS One*, 11, e0156620, 2016.
- McMillan and Schwertmann: Morphological and genetic relations between siderite, calcite and goethite in a Low Moor Peat from southern Germany, *Eur. J. Soil Sci.*, 49, 283–293, <https://doi.org/10.1046/j.1365-2389.1998.00154.x>, 1998.
- 320 Montaña López, F., Kukkadapu, R., and Hicks Pries, C.: Mössbauer spectroscopy dataset of Arctic permafrost soils in Alaska (2023–2025), <https://doi.org/10.18739/A2R49GB9D>, 2026a.
- Montaña López, F., Landis, J. D., Wilkins, S. D., Schaefer, S. R., Kukkadapu, R., Fromm, S. F. von, Grandy, S., Ernakovich, J., and Pries, C. H.: Organo-mineral interactions in active layer and permafrost soils along aging Arctic landscapes in Alaska (2021–2024), <https://doi.org/10.18739/A2VX0653D>, 2026b.
- 325 Natali, C., Bianchini, G., and Carlino, P.: Thermal stability of soil carbon pools: Inferences on soil nature and evolution, *Thermochim. Acta*, 683, 178478, <https://doi.org/10.1016/j.tca.2019.178478>, 2020.
- Ping, C. L., Bockheim, J. G., Kimble, J. M., Michaelson, G. J., and Walker, D. A.: Characteristics of cryogenic soils along a latitudinal transect in arctic Alaska, *J. Geophys. Res. Atmos.*, 103, 28917–28928, <https://doi.org/https://doi.org/10.1029/98JD02024>, 1998.
- 330 Postma, D.: Formation of siderite and vivianite and the pore-water composition of a Recent bog sediment in Denmark, *Chem. Geol.*, 31, 225–244, [https://doi.org/10.1016/0009-2541\(80\)90088-1](https://doi.org/10.1016/0009-2541(80)90088-1), 1980.
- Postma, D.: Pyrite and siderite formation in brackish and freshwater swamp sediments, *Am. J. Sci.*, 282, 1151–1183, 1982.
- Poulton, S. W. and Canfield, D. E.: Development of a sequential extraction procedure for iron: implications for iron partitioning in continentally derived particulates, *Chem. Geol.*, 214, 209–221, <https://doi.org/10.1016/j.chemgeo.2004.09.003>, 2005.
- 335 Rancourt, D. G. and Ping, J. Y.: Voigt-based methods for arbitrary-shape static hyperfine parameter distributions in Mössbauer spectroscopy, *Nucl. Instruments Methods Phys. Res. Sect. B Beam Interact. with Mater. Atoms*, 58, 85–97, [https://doi.org/10.1016/0168-583X\(91\)95681-3](https://doi.org/10.1016/0168-583X(91)95681-3), 1991.
- Ristić, M., Krehula, S., Reissner, M., and Musić, S.: 57Fe mössbauer, XRD, FT-IR, FE SEM analyses of natural goethite, hematite and siderite, *Croat. Chem. Acta*, 90, <https://doi.org/10.5562/cca3233>, 2017.
- 340 Roh, Y., Zhang, C.-L., Vali, H., Lauf, R. J., Zhou, J., and Phelps, T. J.: Biogeochemical and environmental factors in Fe



- biomineralization: magnetite and siderite formation, *Clays Clay Miner.*, 51, 83–95, <https://doi.org/10.1346/CCMN.2003.510110>, 2003.
- Rooney, E. C., VanderJeugd, E., Avasarala, S., Miah, I., Berens, M. J., Kinsman-Costello, L., Weintraub, M. N., and
345 Herndon, E. M.: Decoupling of redox processes from soil saturation in Arctic tundra, *Commun. Earth Environ.*, 5, 746, <https://doi.org/10.1038/s43247-024-01927-1>, 2024.
- Rothwell, K. A., ThomasArrigo, L. K., Kaegi, R., and Kretzschmar, R.: Low molecular weight organic acids stabilise siderite against oxidation and influence the composition of iron (oxyhydr)oxide oxidation products, *Environ. Sci. Process. Impacts*, 27, 133–145, <https://doi.org/10.1039/D4EM00363B>, 2025.
- 350 Sánchez-Román, M., Fernández-Remolar, D., Amils, R., Sánchez-Navas, A., Schmid, T., Martin-Uriz, P. S., Rodríguez, N., McKenzie, J. A., and Vasconcelos, C.: Microbial mediated formation of Fe-carbonate minerals under extreme acidic conditions, *Sci. Reports* 2014 41, 4, 4767–, <https://doi.org/10.1038/srep04767>, 2014.
- Schädel, C., Schuur, E. A. G., Bracho, R., Elberling, B., Knoblauch, C., Lee, H., Luo, Y., Shaver, G. R., and Turetsky, M. R.: Circumpolar assessment of permafrost C quality and its vulnerability over time using long-term incubation data, *Glob. Chang. Biol.*, 20, 641–652, <https://doi.org/10.1111/gcb.12417>, 2014.
- 355 Schuur, E. A. G., Abbott, B. W., Commane, R., Ernakovich, J., Euskirchen, E., Hugelius, G., Grosse, G., Jones, M., Koven, C., Leshyk, V., Lawrence, D., Lorant, M. M., Mauritz, M., Olefeldt, D., Natali, S., Rodenhizer, H., Salmon, V., Schädel, C., Strauss, J., Treat, C., and Turetsky, M.: Permafrost and Climate Change: Carbon Cycle Feedbacks From the Warming Arctic, *Annu. Rev. Environ. Resour.*, 47, 343–371, <https://doi.org/10.1146/annurev-environ-012220-011847>, 2022.
- 360 Sowers, T. D., Wani, R. P., Coward, E. K., Fischel, M. H. H., Betts, A. R., Douglas, T. A., Duckworth, O. W., and Sparks, D. L.: Spatially Resolved Organomineral Interactions across a Permafrost Chronosequence, *Environ. Sci. Technol.*, 54, 2951–2960, <https://doi.org/10.1021/acs.est.9b06558>, 2020.
- Thompson, A., Byrne, J. M., Dreher, C. L., Grigg, A. R. C., Joshi, P., Latta, D. E., Neumann, A., Notini, L., O’Neill, K. E. B., and Rothwell, K. A.: Current Practices for Analyzing Soils and Sediments via Mössbauer Spectroscopy, *J. Plant Nutr. Soil Sci.*, 188, 742–773, <https://doi.org/10.1002/JPLN.12024>, 2025.
- 365 Vuillemin, A., Wirth, R., Kemnitz, H., Schleicher, A. M., Friese, A., Bauer, K. W., Simister, R., Nomosatryo, S., Ordoñez, L., Ariztegui, D., Henny, C., Crowe, S. A., Benning, L. G., Kallmeyer, J., Russell, J. M., Bijaksana, S., Vogel, H., and Team, the T. D. P. S.: Formation of diagenetic siderite in modern ferruginous sediments, *Geology*, 47, 540–544, <https://doi.org/10.1130/G46100.1>, 2019.
- 370 Vuong, T. X., Heitkamp, F., Jungkunst, H. F., Reimer, A., and Gerold, G.: Simultaneous measurement of soil organic and inorganic carbon: evaluation of a thermal gradient analysis, *J. Soils Sediments*, 13, 1133–1140, <https://doi.org/10.1007/s11368-013-0715-1>, 2013.
- Walker, D. A., Auerbach, N. A., Bockheim, J. G., Chapin, F. S., Eugster, W., King, J. Y., McFadden, J. P., Michaelson, G. J., Nelson, F. E., Oechel, W. C., Ping, C. L., Reeburg, W. S., Regli, S., Shiklomanov, N. I., and Vourlitis, G. L.: Energy and
375 trace-gas fluxes across a soil pH boundary in the Arctic, *Nature*, 394, 469–472, <https://doi.org/10.1038/28839>, 1998.

<https://doi.org/10.5194/egusphere-2026-2641>

Preprint. Discussion started: 22 May 2026

© Author(s) 2026. CC BY 4.0 License.



Xiong, W., Wells, R. K., and Giammar, D. E.: Carbon Sequestration in Olivine and Basalt Powder Packed Beds, *Environ. Sci. Technol.*, 51, 2105–2112, <https://doi.org/10.1021/acs.est.6b05011>, 2017.

Zosel, J., Oelßner, W., Decker, M., Gerlach, G., and Guth, U.: The measurement of dissolved and gaseous carbon dioxide concentration, *Meas. Sci. Technol.*, 22, 72001, <https://doi.org/10.1088/0957-0233/22/7/072001>, 2011.

380